J. Indian Chem. Soc.,
Vol. 97, No. 9b, September 2020, pp. 1487-1497

Identification of the inorganic constituents in urinary stones using powder-XRD, FT-IR, FE-SEM, EDX and HR-TEM and structural characterization using powder-XRD data

Ridhdhi laiya[a,b], Pragnya A. Bhatt[a] and Parimal Paul*[a,b]

[a]Analytical and Environmental Science Division and Centralized Instrument Facility, CSIR-Central Salt and Marine Chemicals Research Institute, G.B. Marg, Bhavnagar-364 002, Gujarat, India

[b]P. D. Patel Institute of Applied Sciences, Charotar University of Science and Technology, Changa-388 421, Gujarat, India

E-mail: ppaul@csmcri.res.in

Manuscript received online 09 July 2020, accepted 30 August 2020

Urinary stone related diseases is an acute and common problem across the world. However, causes of its formation/recurrence and possible treatment to prevent its formation are yet to be fully understood. Therefore, analysis of the mineralogical constituents of the urinary stones and its correlation with patient's food habit, metabolic disorder and other regional factors is important. With advancement in instrument based analytical techniques, precise analysis of the stone constituents is achievable. For this purpose, ten urinary stones were collected from local patients (Gujarat, the western part of India) through physician/hospital sources and were analyzed using powder-XRD, FT-IR, FE-SEM, HR-TEM and EDX analysis. Major constituents found are whewellite and weddellite (calcium oxalate monohydrate and dihydrate) and a minor constituent found is calcite. EDX analysis has quantified the amount of metal ion, carbon and oxygen present in the constituents. PXRD data were used for phase identification and quantification with the aid of JCPDS No., it has also provided crystallite size and strain. PXRD data has also used for identification of crystal system and to calculate unit cell parameters. Structural characterization of two of the COM samples were carried out and Rietveld refinement has been done using PXRD data. SEM and TEM images have provided morphological characterization of the stones. All of these results are presented herein.

Keywords: Urinary stone, powder-XRD, structure determination, Rietveld method, HR-TEM.

Introduction

Urolithiasis is considered as a serious medical problem worldwide because of its adverse effect on human health, which is increasing day by day[1]. A large number of population has been suffering from urolithiasis and many of these patients may lose kidney or may result renal damage[2]. Despite life threatening disease with high recurrence rate, it has not been studied extensively and to deal with this, it is important to understand its constituents, its mechanism of formation and how its constituents change with other factors such as food habit and environment. Some progress has been made in this direction, as may be seen the report on mechanistic aspects of its formation[3] and studies related to various factors such as medicinal[4], regional specificities[1,5], therapeutic[6], etc., which influence its formation. To understand mechanism of formation and its prevention, it is important to know the bio-mineral constituents of the urinary stones and some work on it have also been reported[7–9]. However, mechanism of stone formation process *in vivo* and *in vitro* is not yet fully understood and not any treatment is available to prevent the occurrence of the urinary stone disease in human beings.

The analysis of kidney stones so far revealed that calcium oxalate with variable number of water molecule of crystallization is the main constituents of the urinary stones, it exists in three forms i.e. whewellite, weddellite and caoxite, which are calcium oxalate with one, two and three water molecules, respectively. Calcium oxalate monohydrate (COM) and calcium oxalate dihydrate (COD) are found as the most common constituents of kidney stones[10]. Presence of calcium oxalate trihydrate (CaOx) has also been reported and the factors such as hypercalciuria, hyperoxaluria, crystal promoters and inhibitors, low urine volume etc. apparently assist CaOx crystallization[11–14]. Recently, one research group

has reported that amorphous calcium phosphate plays an important role in the nucleation of CaOx stone by promoting the aggregation of amorphous CaOx precursors at early induction times[15]. It has also been reported that calcium carbonate crystals promote crystallization of calcium oxalate[16]. Therefore, inhibition of calcium carbonate crystal formation in Henle's loop might play an important role in the prevention of calcium oxalate stone formation[16]. Therefore, detail analysis of the constituents of urinary stones of different category/sources with different history/background of the patients is essential. Large number of data with variety of samples will contribute towards better understanding of mechanism and prevention of its formation.

For absolute characterization of a pure phase from powder-XRD data, Rietveld refinement method is an important technique for structure determination and refinement and also for quantification of mixed phase constituents[17,18]. However, studies related to the application of Rietveld refinement for a monophasic urinary stone constituent is not many[19], though this method is one of the most suitable one for structure refinement of the polycrystalline monophasic constituent phase of urinary stone.

In the present study, urinary stones from ten local patients (Gujarat state, western India) have been analyzed using powder-XRD. Quantification of the constituents was carried out using the Rietveld refinement technique. Crystallite size, lattice strain and crystallinity analysis were carried out using High score plus software. Structure refinement of pure COM phase was performed for two selected urinary stones using the Rietveld refinement method. FT-IR analysis was carried out to identify the constituents and also as supportive evidence to PXRD findings. EDX analysis was carried out to confirm the metal and other elements present in the stones and also for their quantification. FE-SEM and HR-TEM images were recorded to examine the morphology and topography of the urinary stones.

Experimental

Sample preparation:

Urinary stones used in the present study were collected from the local (Gujarat, India) patients suffering from kidney stone disease. The stones were removed from the patients surgically by the medical surgeons and a few cases it was removed naturally. The collected urinary stones were cleaned with water and were dried at room temperature for two weeks. For analysis, the samples were properly grounded using a pestle and mortar and tried to make uniform grain size.

Instrumental measurement:

IR spectra were recorded on a Perkin-Elmer instrument, model spectrum GX FT-spectrometer using KBr pellets. Powder-XRD measurements were performed on PANalytical Empyrean series 2 Powder X-ray diffractometer, model no. DY1251 (PIXcel 3D detector) using Ni-filter, Cu-Kα monochromatic radiation (λ = 1.54 Å) at ambient temperature (298 K). SEM images were recorded on a JSM-7100F Field Emission Scanning Electron Microscope (FE-SEM) with 15 kV LED operation voltage. To make the sample conductive, it was coated with 15 nm thickness of gold using a sputter coater and then the images were recorded. Elemental analysis was carried out using Energy Dispersive X-ray (EDX) system from Oxford Instruments, model: X-max^N, coupled with FE-SEM. TEM images were recorded on a Joel made JEM-2100 (model) instrument. Samples for TEM analysis was prepared by dispersing the samples on the C-coated Cu grid, followed by drying it at the ambient temperature and finally used it for recording images.

Structure determination from PXRD data:

For structure determination, good quality and accurate PXRD data were collected and then search-match analysis was performed for the samples for structure determination. For this purpose, standard calcium oxalate monohydrate (COM) sample was obtained from Fluka Sigma-Aldrich Chemie Company. The powder-XRD data were recorded for each of the calculus in the diffraction angle range of 10°– 80° 2θ with 0.0131° (2θ) step size and counting time of 298.095 s at the voltage of 40 kV and 30 mA. The search-match analysis was carried out for each of the obtained diffraction pattern of stones using ICDD (International Centre for Diffraction Data) and JCPDS (Joint Committee on Powder Diffraction Standards) database in High score plus software and constituent of each of the urinary stone was determined. Constituent matched phase for both the stones for structure determination was COM having JCPDS number 98-024-6802. This phase was used as an input for Rietveld refinement for the urinary stones. The profile function used for describing the peak shape was a Pseudo-Voigt type and the background was modeled as a polynomial or available background. Structure fitting mode of the Rietveld refinement has been em-

ployed for further analysis. The Rietveld method uses the least squares approach to refine a theoretical line profile using the assumed phase until it matches the measured profile. Profile variables (U, V, W, peak shape 1 and 2), global variables (background coefficient, zero shifts), structural parameters (cell, atomic co-ordinates), preferred orientations and scale factor were refined and reasonable estimates were obtained for the same. Refinement was carried out for the urinary stones and also for standard COM (STD-COM) and the best fit between calculated and observed patterns was obtained for each of the refinement. The best fit was assessed by the parameter goodness of fit (GOF). The value of this parameter should be less than or equal to five. GOF is expressed in terms of other reliability index parameters (R_p, R_{wp} and R_{exp}) which are used as indicators for the evaluation of refinement[20].

$$GOF = \frac{R_{wp}}{R_{exp}} \quad (1)$$

where, R_{wp} is weighted R profile and expressed as follows. R_{wp} uses a weighting function to place more emphasis on a good fit between high intensity data points (such as intense peaks) and less emphasis on low intensity data points (such as the background). In a good fit, R_{wp} should be less than 10.

$$R_{wp} = \left[\frac{\Sigma \omega_i \{y_i(obs) - y_i(cal)\}^2}{\omega_i \{y_i(obs)\}^2} \right]^{1/2} \quad (2)$$

R expected (R_{exp}) is a statistical evaluation of the noise of the data. Smaller the value of R_{exp} indicates the better quality data.

$$R_{exp} = \left[\frac{(N - P)}{\omega_t \{y_i(obs)\}^2} \right]^{1/2} \quad (3)$$

where, N is the experimental observations and P is the number of parameters to be fitted. R profile (R_p) is the residual difference between observed and calculated plots.

$$R_p = \frac{\Sigma |y_t(obs) - y_t(cal)|}{\Sigma |y_t(obs)|} \quad (4)$$

Above mentioned parameters is a valuable index to estimate the quality of refinement. After getting a good fit, Fourier map analysis was employed and electron density maps along with the refined structure have been obtained for urinary stones. Atomic distances and atomic angles are calculated for COM constituent of both the urinary stones and for standard COM sample. A combination of Rietveld and Fourier map analysis is proved to be an appropriate tool to refine the structure of the polycrystalline constituent of urinary stones.

Quantification of urinary stone constituents:

A few reports are found in the literature for the quantification of the crystalline components of urinary stones using Rietveld refinement technique[21,22]. Quantification of the mixed phase constituents present in the urinary calculi can be done using the Rietveld method. Quantification of eight urinary stones and a standard COM sample has been performed using Rietveld refinement. Refinement was done in automatic and/or semi-automatic mode using High score plus software. For automatic mode, the background is specified using a suitable polynomial function. However, for semi-automatic mode available background is used. In order to acquire the best fit with experimental powder pattern, during the refinement for each of the sample structural, micro-structural parameters are refined for simulated powder pattern of each of the matched constituent phase/phases of respective stone. Micro-structural parameters namely crystallite size and lattice strain have been evaluated using X-ray Debye-Scherrer equation[22] employed in High score plus software. The formula of the Debye-Scherrer is as follows:

$$L = \frac{K\lambda}{B_m \cos\theta} \quad (5)$$

where, L = average crystallite size, B_m = FWHM of maximum intensity peak, λ = wavelength of X-ray radiation and K = constant related to the crystallite shape and is approximately equal to unity. The best fit is assessed by GOF parameter which (should be less than or equal to five) is generated by refinement procedure. Unit cell parameters and reliability index parameters (R_{exp}, R_p, R_{wp} and GOF) for specified samples and for STD-COM were calculated.

Results and discussion

The procedure for collection of samples was described in the Experimental Section. Samples' code, age of the patient, gender, food habit, stone removal procedure (surgically/naturally removed) are summarized in Table 1.

Table 1. Sample code and some other relevant information of the patients

Sample code	Age	Gender	Food habits	Stone removal procedure
KS-1	24	Female	Vegetarian	Surgically
KS-2	24	Female	Vegetarian	Surgically
KS-3	60	Male	Vegetarian	Surgically
KS-4	56	Female	Vegetarian	Surgically
KS-5	45	Male	Vegetarian	Surgically
KS-6	47	Male	Vegetarian	Surgically (Laser)
KS-7	50	Male	Vegetarian	Naturally removed
KS-8	58	Female	Vegetarian	surgically
KS-9	27	Female	Vegetarian	Surgically
KS-11	40	Male	Vegetarian	Surgically

Powder X-ray diffraction study:

Powder X-ray diffractograms of urinary stones, recorded following the methods described in the Experimental Section, are shown in the Figs. 1 and 2. Fig. 1 shows the diffractograms of six samples, KS-1, KS-2, KS-4, KS-7, KS-8 and KS-9, which contain pure phase of calcium oxalate monohydrate (COM). Fig. 2 displays the diffractograms of five samples, KS-1, KS-3, KS-5, KS-6 and KS-11, containing constituent phases of pure COM, pure COD and mixture of COM and calcite. Identification of the constituents has been made on the basis of JCPDS Number. Quantification of the

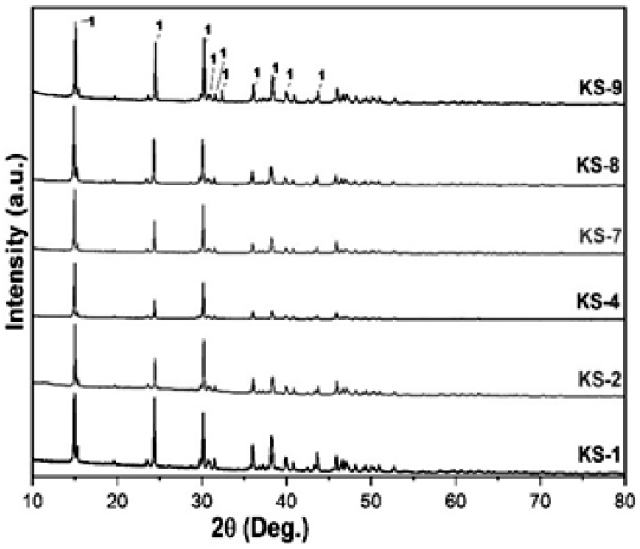

Fig. 1. Diffractograms of six samples containing pure phase of calcium oxalate monohydrate ('1' denotes peak for COM).

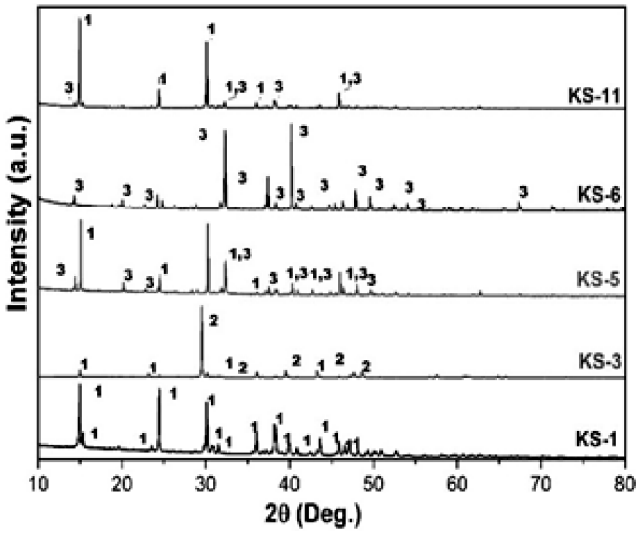

Fig. 2. Diffractograms of five urinary stone samples containing pure as well as mixed phases ('1', '2' and '3' denote peaks for COM, calcite and COD, respectively).

constituents has been made on the basis of Rietveld refinement, as shown in the Fig. 3a and 3b. Fig. 3a (KS-7) shows the presence of monophasic constituent, 100% COM and Fig. 3b (KS-3) shows the presence of mixed phase constituents, 83.0% calcite and 17.0% COM phase. The constituents of the urinary stones were determined on the basis of the search-match analysis, which revealed that out of ten stones analyzed, six (KS-1, KS-2, KS-4, KS-7, KS-8 and KS-9) were found to have calcium oxalate monohydrate as a pure phase constituent, one (KS-6) stone was found to have calcium oxalate dihydrate (COD) as single constituent and remaining three stones (KS-3, KS-5 and KS-11) were found to have mixed phase constituents. KS-3 was having COM phase admixed with calcite whereas KS-5 and KS-11 were found to have COM and COD, calcium oxalate with varied hydration state. Details of the findings with sample code, JCPDS reference number, mineral(s) name, chemical formula, quantification of matched phase, crystallite size (nm) and lattice strain (%) are presented in Table 2.

This crystallite size range matches well with the reported crystallite size for stone constituents in the literature[20]. The crystallite size is intrinsically associated to the growth conditions of the crystalline phases. Therefore, it may be one of the factors which can be correlated to the chemistry of growth

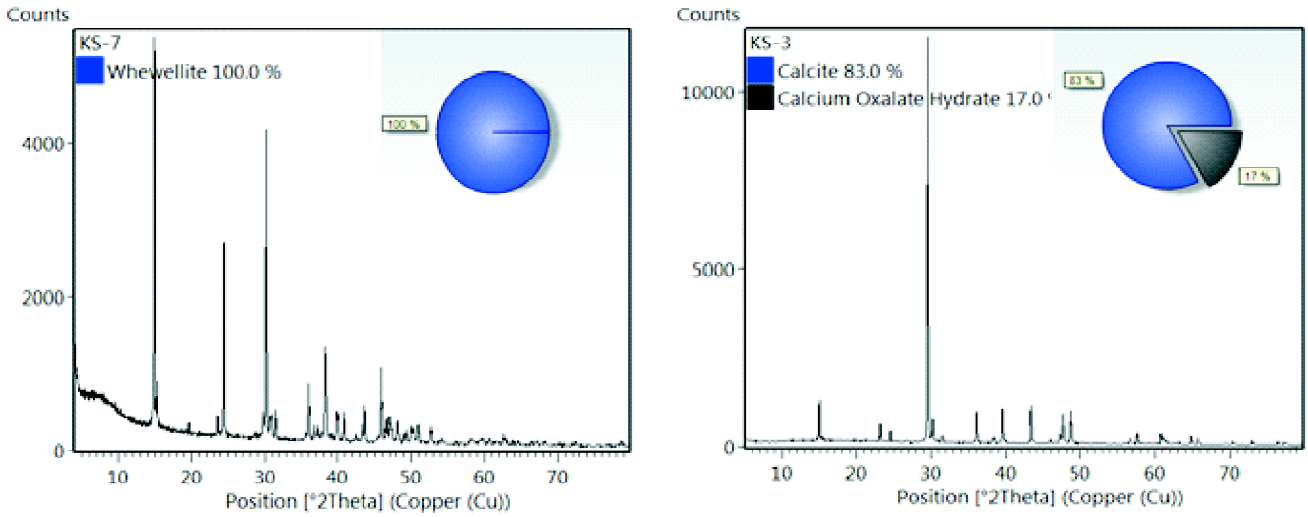

Fig. 3. Quantification of the urinary stone constituents of KS-7 having pure COM and KS-3 having mixed phases, respectively.

Table 2. Findings from PXRD technique for human urinary stone samples

Sample code	JCPDS No.	Matched phases	Chemical formula of matched phase	Quantification (%)	Crystallite size (nm)	Lattice strain
KS-1	98-024-6802	Whewellite	$CaC_2O_4.H_2O$	100	52.8	0.399
KS-2	98-024-6802	Whewellite	$CaC_2O_4.H_2O$	100	53.4	0.641
KS-3	01-085-1108	Calcite	$CaCO_3$	83.0	62.7	0.288
	04-009-6324	Whewellite	$CaC_2O_4.H_2O$	17.0	42.0	0.782
KS-4	98-003-0782	Whewellite	$CaC_2O_4.H_2O$	100	52.7	0.650
KS-5	98-003-0782	Whewellite	$CaC_2O_4.H_2O$	–	178.9	0.132
	04-011-6807	Weddellite	$CaC_2O_4.2H_2O$		75.6	0.183
KS-6	01-083-5347	Weddellite	$CaC_2O_4.2.26H_2O$	100	145.9	0.114
KS-7	98-003-0782	Whewellite	$CaC_2O_4.H_2O$	100	51.0	0.668
KS-8	04-009-6324	Whewellite	$CaC_2O_4.H_2O$	100	37.3	0.869
KS-9	98-015-3499	Whewellite	$CaC_2O_4.H_2O$	100	53.1	0.643
KS-11	98-024-6802	Whewellite	$CaC_2O_4.H_2O$	94.5	96.5	0.410
	01-083-5336	Weddellite	$CaC_2O_4.2.20.H_2O$	5.5	90.0	0.161

medium and thermodynamics, both of which is defined by the metabolism of a patient[23]. Crystallite size depends on the medium in which crystallization occurs, degree of crystallization and other kinetics factors such as nucleation, growth etc.[24]. Crystallite size and strain variation may be attributed to the presence of various urinary solutes in form of promoters, inhibitors etc. affecting the crystallization process of urinary stone. As crystallite size increases the lattice strain decreases. As may be seen from Table 2 that in monophasic COM constituent crystallite size variation is between 178.9 to 37.3 nm. Crystallite sizes of the calcium oxalate dihydrate constituent of the stones vary from 145.9 nm to 75.6 nm. This shows the uniqueness of the medium, its thermodynamic and kinetic conditions provided by the individual patient. X-Ray diffraction is a simpler and easier approach for the determination of precise particle size and lattice strain in microcrystalline samples. Crystal systems, cell parameters and Rietveld refinement parameters of stone constituents are presented in Table 3. All of the COM phase constituent has a monoclinic crystal system with different unit

Table 3. Crystal system, cell parameters and Rietveld refinement parameters of stone constituents and a standard sample (COM)

		Unit cell parameters					Reliability index parameters			
Sample code	Crystal system	*a* (Å)	*b* (Å)	*c* (Å)	β (°)	Vol. (10^6 pm^3)	R_{exp} (%)	R_p (%)	R_{wp} (%)	GOF
KS-1	Monoclinic	10.11	7.26	6.29	109.44	438.14	3.43	6.44	8.93	6.76
KS-2	Monoclinic	10.12	7.30	6.29	109.45	438.60	5.75	7.43	9.59	2.78
KS-3	Monoclinic	10.12	7.30	6.30	109.50	439.51	7.66	14.7	19.94	6.76
KS-4	Monoclinic	6.27	14.56	10.11	109.47	871.80	3.25	8.55	12.86	3.95
KS-7	Monoclinic	6.28	14.58	10.11	109.48	875.06	5.38	7.79	10.10	1.87
KS-8	Monoclinic	10.11	7.29	6.29	109.42	437.81	1.60	5.45	7.31	4.57
KS-9	Monoclinic	6.29	14.58	10.11	109.46	879.90	2.80	6.13	7.97	2.83
KS-11	Monoclinic	10.11	7.29	6.29	109.46	438.00	3.02	7.45	11.0	3.64
COM-STD	Monoclinic	10.11	7.29	6.29	109.42	437.81	7.05	8.99	11.59	2.69

cell parameters. It may be seen from the table that cell volume parameters of COM unit cell are of two types; one type (KS-1, KS-2, KS-3, KS-8, KS-11 and KS-COM) has average unit cell volume 438.31 (10^6 pm^3), which is roughly half of the other type, average 875.58 10^6 pm^3 (KS-4, KS-7 and KS-9). This indicates twinned crystal formation in the second type, which are consist of two or more crystals of the same (or isomorphs) type joined together at a definite mutual orientation[13]. According to a study reported by Petrova *et al.*, COM crystals grow in twin, spherulite, splices and dendrite forms depending on the medium (crystal forming ions in distilled water, in urine, in gel containing medium or in presence of magnesium, iron and aluminum), in which crystals are formed[24].

Structure determination:

Out of seven urinary stones containing pure COM, structure refinement was carried out for two selected urinary stones i.e. KS-1 and KS-2. The observed, calculated and difference plot of the diffraction patterns of these two urinary stones are shown in Fig. 4 and the structure (001 plane) of KS-1 and KS-2 urinary stones are given in Fig. 5. As seen from the

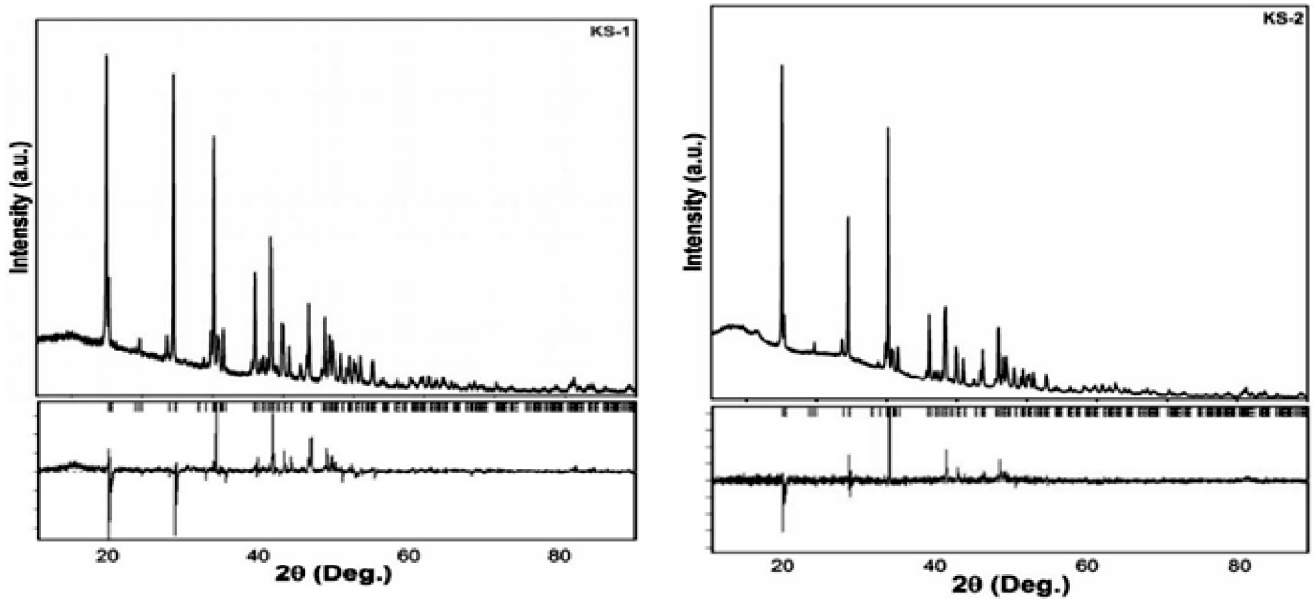

(a) (b)

Fig. 4. Final Rietveld refinement result: observed (solid lines), calculated (dotted lines) and difference plot of the profiles.

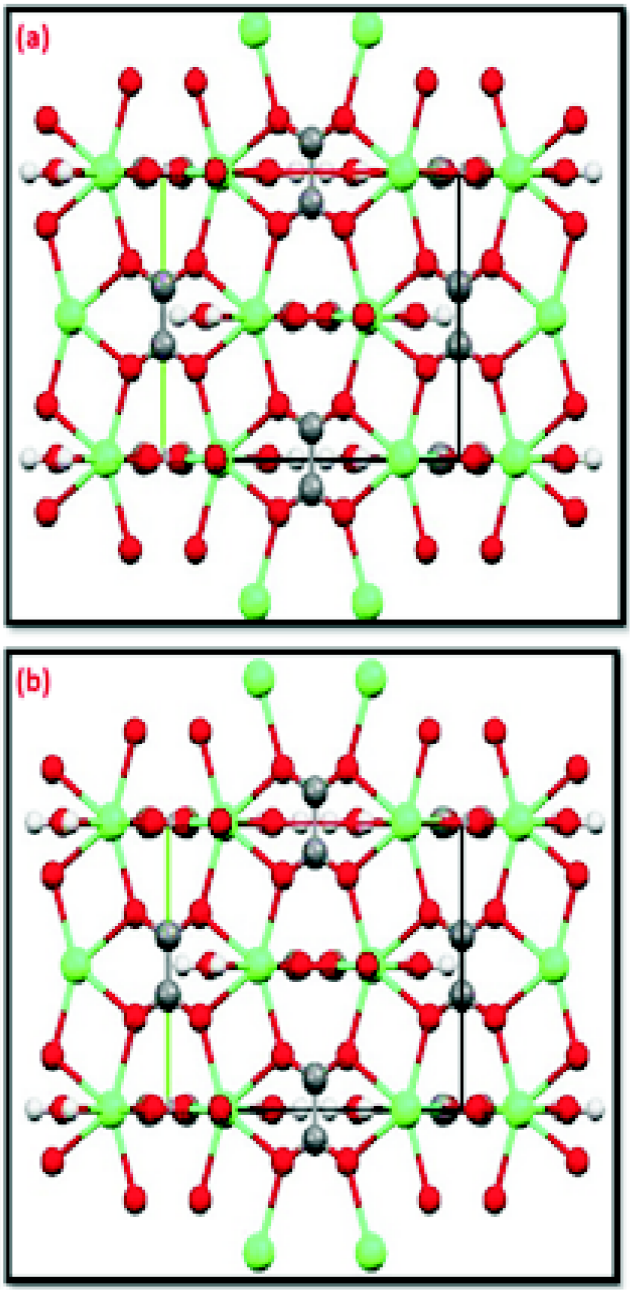

Fig. 5. Structure of COM (green, Ca; red, oxygen and grey, carbon); projected down 001 plane; of two calculi namely (a) KS-1 and (b) KS-2.

figures, calcium atoms are coordinated to the oxygen atoms in the asymmetric unit of COM in KS-1 and KS-2 stones. The Ca-O distance lies in the range 2.425 Å to 2.469 Å with the Ca-Ca separation. Moreover, C-O distance observed in the range of 1.22 Å to 1.25 Å. Each Ca atom coordinated to one water molecule. The bond angles of O-Ca-O and O-C-O lie in the range of 65.13° to 76.44° and 125.9° to 127.23°, respectively. The obtained bond angles and bond distances values are in good agreement with the reported values in the literature[13,25]. Interatomic distances and bond angle parameters for STD-COM, KS-1 and KS-2 are given in the Table 4. Structure of KS-1 and KS-2 are having their uniqueness reflected in their coordination geometry, coordination parameters and angular parameters. This uniqueness depends on, site at which the stone is formed, the variation in ionic strength of constituent phases, varied concentration of presence of stone inhibitors and promoters etc.

Table 4. The bond distances and bond angles of two kidney stones structures using Rietveld analysis

Sr. no.	Distance	COM-std.	KS-1	KS-2
1.	Ca-O1	2.435	2.436	2.437
2.	Ca-O2	2.425	2.426	2.427
3.	Ca-O3	2.468	2.430	2.469
4.	Ca-O4	2.432	2.433	2.454
5.	C1-O4	1.253	1.253	1.253
6.	C2-O2	1.248	1.248	1.248
7.	C2-O3	1.229	1.230	1.230
Sr. no.	Angles	COM-std. (Å)	KS-1 (Å)	KS-2 (Å)
1.	O4-Ca1-O4	75.33	66.49	66.49
2.	O4-Ca1-O1	74.92	74.93	74.93
3.	O2-Ca1-O3	65.13	65.11	76.44
4.	O4-C1-O4	125.99	125.97	125.96
5.	O3-C1-O2	127.21	127.23	127.22

FT-IR study:

IR spectra of the five stone samples were recorded for characterization of the samples and to complement the findings from powder-X-ray study. These spectra are shown in Fig. 6 (KS-1, KS-2, KS-4, KS-7, KS-8) and they exhibited the characteristic bands for COM phase. The strong IR bands at 1620 cm^{-1} and 1317 cm^{-1} correspond to asymmetric and symmetric COO^- stretching vibrations of the coordinated oxalate group. The three weak bands in the fingerprint region at 781, 658 and 517 cm^{-1} are assigned to in-plane O-C=O bending, out-of-plane O-H deformation and CO_2 wagging mode. The broad band in the region 3000 to 3700 cm^{-1} is due to the symmetric and asymmetric O-H stretching modes of the water molecule, which confirms the presence of water molecule(s) as a solvent of crystallization in COM[20]. The band

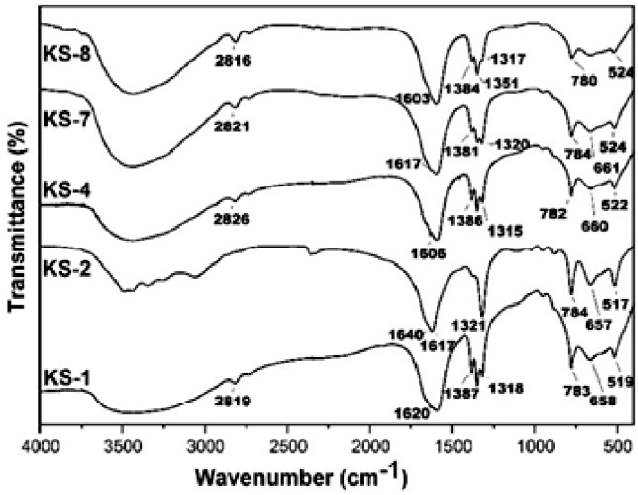

Fig. 6. FT-IR spectra of the stones containing pure COM phase (KS-1, KS-2, KS-4, KS-7 and KS-8).

around 1384 cm^{-1} may be attributed to the C-C bond stretching vibrational mode[26]. In addition, all of these five samples exhibited a strong band in the region 1600–1650 cm^{-1}, which is attributed to the amide moiety present in the urinary stones[27,28].

Scanning electron microscopic study (SEM):

SEM images of six samples were recorded following the method described in the Experimental Section and are shown in Fig. 7. Fig. 7a shows the stacking of rectangular COM crystals having different orientations and smooth surface morphology of KS-2. KS-3 however, shows randomly oriented rod-like crystals (shown by white arrows) and smooth surface (shown by yellow arrows) in the Fig. 7b. Stacking of parallel thin layers of constituent crystallites (with white arrows) is seen in Fig. 7c and Fig. 7f. This morphology of COM is similar to that reported by the research group of Mukherjee[18,19]. Presence of square pyramidal and cylindrical COD crystals (shown by white arrows) and also leukocytes (WBC) (shown by yellow arrows) is evident in the image of KS-6, shown in Fig. 7d[29,30]. Fig. 7e shows the porous morphology of the COD constituent of KS-6, which differs

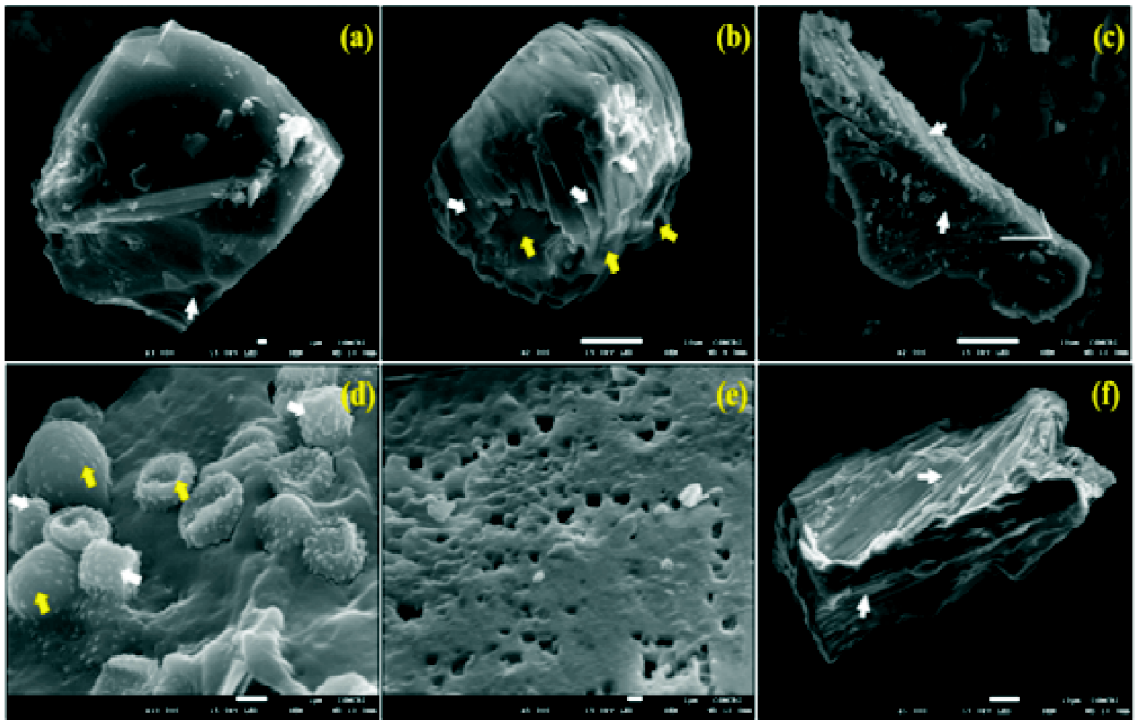

Fig. 7. SEM images of kidney stones (a) KS-2, pure COM with smooth surface morphology, (b) KS-3, with rod-like (white arrow) as well as smooth morphology (yellow arrow), (c) KS-5, with stacking of COM layers, (d) KS-6, square pyramidal or cylindrical COD crystals (shown by white arrows) and leukocytes (WBC) (shown by yellow arrows), (e) KS-6 with COD constituent shows porous morphology and (f) KS-7, pure COM with outer part showing parallel stacking of COM layers.

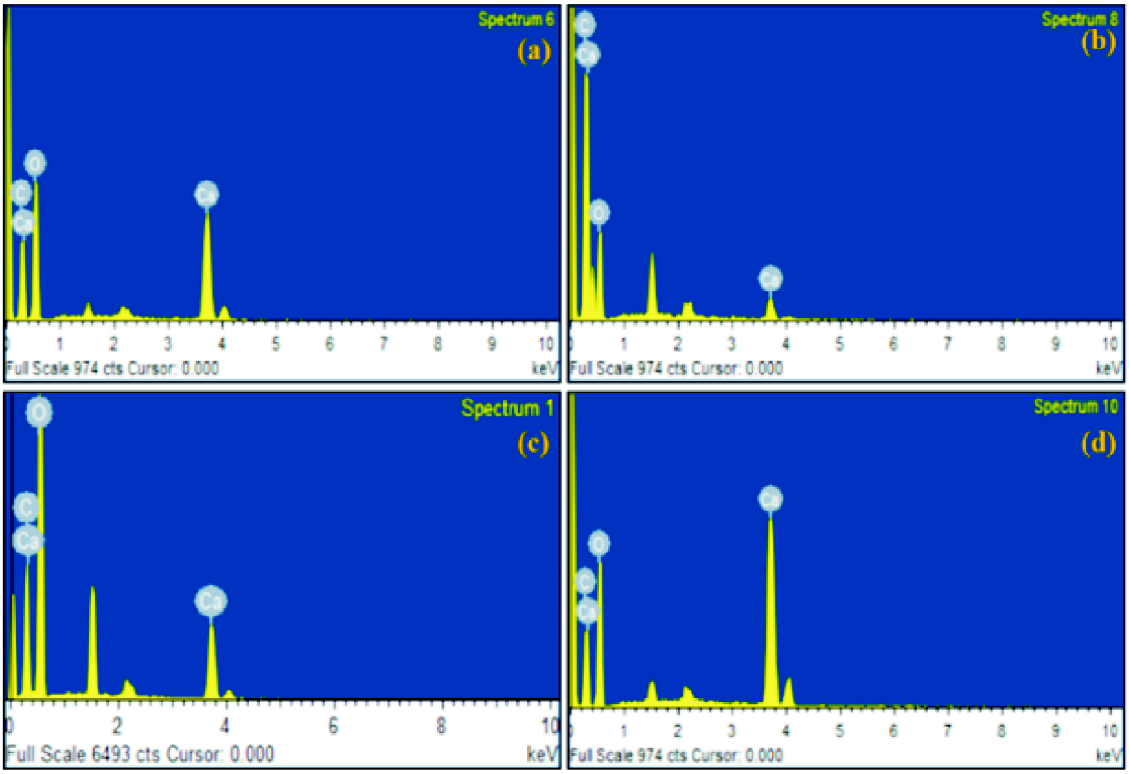

Fig. 8. EDX analysis of urinary stone samples (a) KS-2 calculi, (b) KS-3 calculi, (c) KS-6 calculi and (d) KS-8 calculi.

from usual square pyramidal morphology reported for COD crystals[31].

EDX analysis:

Energy dispersive X-ray analysis (EDX) was performed for most of the samples. EDX profile of four of the samples, namely KS-2, KS-3, KS-6 and KS-8 are shown in the Fig. 8. This analysis shows the presence of Ca, C and O as major elements and it gives complimentary support to the PXRD and FT-IR findings. Table 5 shows the weight % of the elements present in the urinary stones. Presence of varied amount of carbon and calcium content gives evidence of interwoven organo-mineral morphology of respective urinary stone.

Transmission electron microscopic study:

HR-TEM images of six samples were recorded following the method described in the Experimental Section and the images are shown in Fig. 9. Selected area electron diffraction (SAED) of some of the samples were also recoded to investigate the crystallites of the stone and are shown as inset of the TEM images, the rings of which show polycrystalline and also amorphous nature of the stone. It may be noted that the particles in all images are not of uniform size and shape and its degree of aggregation also varies significantly. In few samples, the lattice fringes of the high resolution images (KS-5 and KS-6), which are well-defined parallel atomic planes of the crystallites, are clearly visible. Aggregation of these crystallites may be because of their shape, size and the environment/medium in which it has been formed. It is easier for the particles of small size to aggregate because of their high interface energy[32]. Rapid agglomeration of the urinary crystallites may also occur in the urine environment.

Table 5. Weight % of Ca, O and C from EDX data

Sample code	Weight % of Ca	Weight % of O	Weight % of C
KS-1	20.08	61.63	18.69
KS-2	21.75	58.20	20.05
KS-3	4.10	43.40	52.49
KS-4	30.62	50.35	19.03
KS-6	10.85	65.80	23.35
KS-7	14.09	62.44	23.47
KS-8	30.66	54.34	15.00

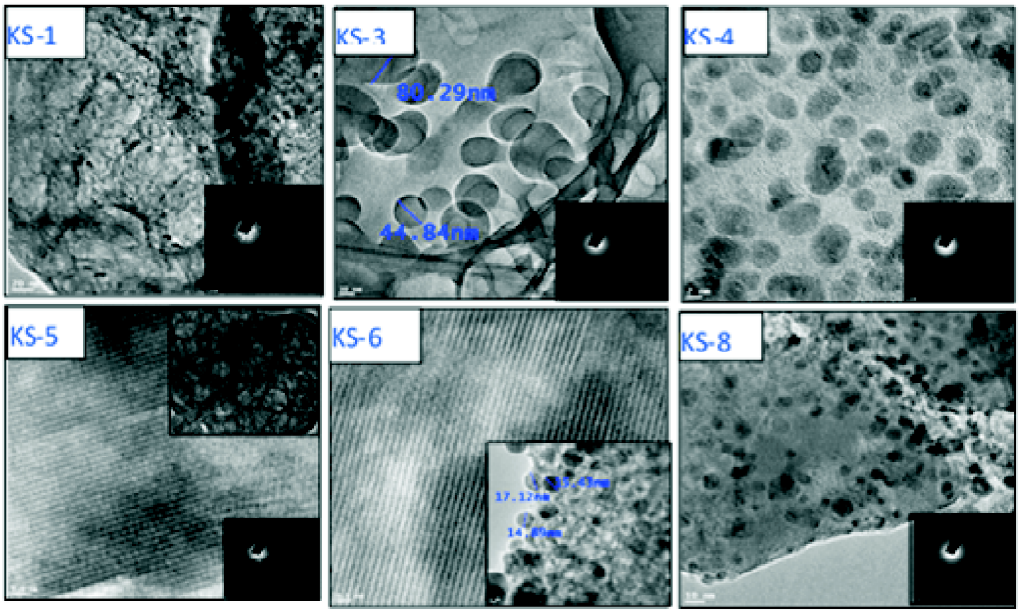

Fig. 9. TEM images of KS-1, KS-3, KS-4, KS-5, KS-6 and KS-8. Selected area electron diffraction (SAED) of five samples are shown as inset. For KS-5 and KS-6, high resolution lattice fringes are also shown.

The analysis of urinary stones revealed the chemical composition of the mineral constituents and morphology. Calcium oxalate monohydrate is the major phase constituent found in the urinary stones analyzed. Patients having COM and/or COD containing urinary stones might be having hypercalciuria, hyperoxaluria, hyperuricosuria and hypocitraturia physiological conditions along with low urine tendency[33]. These patients may have the presence of apatite in their urine causing rapidness in COM nucleation phenomena[15]. Nutritional or medicinal therapeutic strategy taking care of these physiological conditions may prevent recurrence of urinary stone in the respective patient. It has been reported that neutral pH promotes transformation of amorphous calcium carbonate into calcite through a dissolution/reprecipitation mechanism[34]. Magnesium is considered as a provider of increased stability to amorphous calcium carbonate[34]. Therefore, the probable presence of amorphous calcium carbonate and magnesium in urine might be there in the patient having calcite as one of the urinary stone constituents.

Twinned crystal growth observed may be attributed to the presence of some impurities in the surrounding medium causing unequal distributed stresses[35]. In addition to this, the presence of unequal size of crystals and the presence of unstable or metastable forms may also result into twinned growth[36]. Twin and parallel growth occurs most frequently in monoclinic or orthorhombic systems. Although layered growth is the tendency of twinned crystal, it is interesting to note that both types of crystals are having morphology in the form of layered stacking. Porous morphology of COD indicates the presence of amorphous apatite during nucleation of COD crystals.

Conclusions

Mineralogical constituents of ten urinary stone samples have been analyzed on the basis of PXRD, FT-IR, FE-SEM, EDX and HR-TEM. PXRD analysis revealed that out of ten stones analyzed, six are found to have calcium oxalate monohydrate as a pure phase, one stone is found to have calcium oxalate dihydrate as a pure phase and remaining three stones contain mixed phase constituents. From PXRD data, crystal system, unit cell parameters, reliability index parameters, crystallite size and lattice strain are calculated. Structures of two of the calcium oxalate monohydrate samples are determined and refined using the Rietveld refinement and satisfactory data, comparing the standard sample, are obtained. IR data are nicely complemented the chemical composition of the constituents found from PXRD analysis. Morphology of the stones are investigated with the aid of FESEM and the

elemental analysis has been done using EDX, coupled with FE-SEM. Crystallinity, particle size and shape, their arrangement, degree of aggregation are investigated by FE-SEM and HR-TEM, which are good techniques for morphological characterization.

Acknowledgements

We thank Mr. Vinod Agarwal for recording IR spectra, Mr. Jayesh Chaudhari for recording FE-SEM images and EDX analysis and Dr. Gopalram Bhadu for recording TEM images. We also thank Council of Scientific and Industrial Research (CSIR), New Delhi for generous support towards infrastructures and core competency development.

References

1. V. Romero, H. Akpinar and D. G. Assimos, *Rev. Urol.,* 2010, **12**, 86.
2. H. N. Sofia, K. Manickavasakam and T. M. Walter, *Glob. J. Res. Anal.*, 2016, **5**, 183.
3. M. Tsujihata, *Int. J. Urol.,* 2008, **15**, 115.
4. P. N. Panigrahi, S. Dey and S. C. Jena, *Asian J. Anim. Vet. Adv.*, 2016, **11**, 9.
5. M. López and B. Hoppe, *Pedia. Nephrol.*, 2010, **25**, 49.
6. K. V. Chakradhar and S. D. Rao, *Inter. Ayur. Med. J.*, 2013, **1**, 30.
7. V. K. Singh and P. K. Rai, *Biophys. Rev*., 2014, **6**, 291.
8. K. Ramaswamy, D. W. Killilea, P. Kapahi, A. J. Kahn, T. Chi and M. L. Stoller, *Nat. Rev. Urol*., 2015, **12**, 543.
9. A. Gervasoni, P. Primiano, A. Ferraro, G. Urbani, Gambaro and S. Persichilli, *J. of Chemi.,* 2018, **2018**, 1.
10. S. Ranabir, M. P. Baruah and K. R. Devi, *Indian J. of Endocrinol. and Metabol.*, 2012, **16**, 228.
11. V. N. Ratkalkar and J. G. Kleinman, *Clin. Rev. Bone Miner. Metab.,* 2011, **9**, 187.
12. V. A. Finkielstein and D. S. Goldfarb, *CMAJ*, 2006, **174**, 1407.
13. V. Tazzoli and C. Domeneghetti, *American Mineralogisl*, 1980, **65**, 327.
14. D. Aquilano and M. Franchini-Angela, *Phys. Chem. Minerals*, 1981, **7**, 124.
15. B. Xie, T. J. Halter, B. M. Borah and G. H. Nancollas, *Cryst. Growth Des.,* 2015, **15**, 204.
16. S. Geider, B. Dussol, I. S. Nitsche, S. Veesler, P. Berth~z~ne, P. Dupuy, J. P. Astier, R. Boistelle, Y. Berland, J. C. Dagorn and J. M. Verdier, *Calcif. Tissue Int.*, 1996, **59**, 33.
17. K. A. Selevich, L. S. Ivashkevich, A. F. Selevich and A. S. Lyakhov, *Russian J. of Inorg. Chemi.*, 2002, **47**, 1533.
18. A. K. Mukherjee, *J. Indian Inst. of Sci.*, 2007, **87**, 221.
19. A. K. Mukherjee, *J. Indian Inst. of Sci.*, 2014, **94**, 35.
20. P. Chatterjee, A. Chakraborty and A. K. Mukherjee, *Spectrochim. Acta A: Mol. Biomol. Spectrosc.*, 2018, **200**, 33.
21. M. Daudon, D. Bazin, G. André, P. Jungers, A. Cousson, P. Chevallier, E. Véron and G. Matzen, *J. Appl. Cryst*., 2009, **42**, 109.
22. M. T. D. Orlando, L. Kuplich D. O., de Souza, H. Belich, J. B. Depianti, C. G. P. Orlando, E. F. Medeiros, P. C. M. da Cruz, L. G. Martinez, H. P. S. Corrêa, and R. Ortiz, *Powder Diffr. Suppl.,* 2008, **23**, 59.
23. V. Uvarov, I. Popov, N. Shapur, T. Abdin, O. N. Gofrit, D. Pode and M. Duvdevani, *Environ. Geochem. Health*, 2011, **33**, 613.
24. E. V. Petrova, N. V. Gvozdev and L. N. Rashkovich, *J. Optoelectro and Adv. Mater.*, 2004, **6**, 261.
25. T. Echigo, M. Kimata, A. Kyono, M. Shimizu and T. Hatta, *Mineralogical Magazine*, 2005, **69**, 77.
26. V. K. Singh, B. S. Jaswal, J. Sharma and P. K. Rai, *X-Ray Spectrom.*, 2017, **46**, 283.
27. P. Bhatt, and P. Paul, *J. Chem. Sci*., 2008, **120**, 267.
28. V. Asyana, F. Haryanto, L. A. Fitri, T. Ridwan, F. Anwary and H. Soekersi, *J. Phy. Confer. Seri.,* 2016, **694**, 012051.
29. L. V. Didenko, E. R. Tolordava, T. S. Perpanova, N. V. Shevlyagina, T. G. Borovaya, Yu. M. Romanova, M. Cazzaniga, R. Curia, M. Milani, C. Savoia and F. Tatti, *J. Appl. Med. Sci.,* 2014, **3**, 19.
30. Y. M. F. Marickar, P. R. Lekshmi, L. Varma and P. Koshy, *Urol. Res.,* 2009, **37**, 277.
31. M. Racek, J. Racek and I. Hupáková, *Scandi. J. clin. and labora. Investi.*, 2019, **79**, 208.
32. J. Gao, J. Xue, M. Xu, B. Gui, F. Wang and J. Ouyang, *Int. J. Nanomedicine,* 2014 **9**, 4399.
33. V. Sodimbaku and L. Pujari, *Int. J. Pharm. Pharm. Sci.,* 2014, **6**, 23.
34. J. D. Rodriguez-Bianco, S. Shaw, P. Bots, T. Roncal-Herrero and L. G. Benning, *J. Alloys Compd.*, 2012, **536**, 477.
35. J. W. Mullin, "Crystallization", Butterworths & Co. Limited, London, 1961, 18.
36. A. V. Hook, "Crystallization – Theory and Practice", Reinhold Publishing Corporation, New York, 1961, 228.